

Optimization of cultivation conditions for combined nutrient removal and CO₂ fixation in a batch photobioreactor

Ahmed M.D. Al Ketife¹, Simon Judd^{2,3} and Hussein Znad^{1,*}

¹Department of Chemical Engineering, Curtin University; ²Gas Processing Centre, Qatar University; ³Cranfield Water Science Institute, Cranfield University

*corresponding author

Abstract

Background

The application of *Chlorella vulgaris* for simultaneous CO₂ biofixation and nutrient removal has been optimised using response surface methodology (RSM) based on Box Behnken design (BBD). Experimental conditions employed comprised CO₂ concentrations ($C_{c,g}$) of 0.03-22% CO₂, irradiation intensities (I) of 100-400 μ E, temperatures of 20-30°C and nutrient concentrations of 0-56 and 0-19 mg/L nitrogen and phosphorus respectively, the response parameters being specific growth rate μ , CO₂ uptake rate R_c and %nutrient removal.

Results

Over 10-days the biomass concentration reached almost 3 gL⁻¹ for $C_{c,g}$ of 5% CO₂, with corresponding values of 0.74 g L⁻¹ d⁻¹ and 1.17 day⁻¹ for R_c and μ respectively and 100% nutrient (N and P) removals. At 22% CO₂ the R_c and μ decreased by around an order of magnitude, and nutrient removal also decreased to 79% and 50% for N and P respectively.

Conclusion

Optimum values 5% CO₂, 100 μ E and 22°C were identified for $C_{c,g}$, I and T respectively, with μ and R_c reaching 1.53 day⁻¹ and 1 g L⁻¹ d⁻¹ respectively along with associated nutrient

This article has been accepted for publication and undergone full peer review but has not been through the copyediting, typesetting, pagination and proofreading process, which may lead to differences between this version and the Version of Record. Please cite this article as doi: 10.1002/jctb.5084

removal of 100%. Regression analysis indicated a good fit between experimental and model data.

Keywords: Algae; *Chlorella vulgaris*; Photobioreactor; Box-Behnken; optimisation.

Nomenclatures

<u>Symbol</u>	<u>Description and units</u>
$C_{c,g}$	CO ₂ concentration in the inlet gas, %
I	Light incident, $\mu\text{E m}^{-2}\text{s}^{-1}$
P_x	Biomass productivity, $\text{g L}^{-1} \text{d}^{-1}$
R_c	CO ₂ uptake rate, $\text{g L}^{-1} \text{d}^{-1}$
R_c'	Biomass-normalised CO ₂ fixation rate, $\text{g CO}_2 \text{ g biomass}^{-1} \text{d}^{-1}$
T	Temperature, °C
TC	Total carbon, mg L^{-1}
TN	Total Nitrogen concentration, mg L^{-1}
TP	Total Phosphorus concentration, mg L^{-1}
X	Biomass concentration, g L^{-1}

Greek characters

μ Specific growth rate, d^{-1}

Subscripts

i Initial value

f Final value

max Maximum

Abbreviations

ANOVA Analysis of variance

BBD	Box Behnken Design
BNR	Biological nutrient removal
DDF	Derringer's desired function
df	degree of freedom
HRT	Hydraulic residence time, d
MLA	Marine labs American society of microbiology-derived medium
PBR	Photobioreactor
RE	Removal efficiency, %
OC	Organic carbon, mg L ⁻¹

1 Introduction

Microalgae, configured as photobioreactors (PBRs), have attracted considerable attention as the basis of combined biological method for removal of nutrients (nitrogen N and phosphorus P) from wastewaters and CO₂ fixation from flue gases.¹ The microalgae *Chlorella vulgaris* has been extensively studied for CO₂ mitigation under a range of operating conditions, including gas CO₂ concentration,²⁻⁶ light intensity^{7,8} and temperature.^{8,9} Nutrient removal using microalgae has been studied since the mid-1970s.¹⁰ PBRs offer a more sustainable alternative to the established biological nutrient removal (BNR) process, which demands energy for aeration and the pumping of sludge between various tanks in the treatment scheme, as well as supplementary chemical dosing with coagulants to obtain the required P removal.¹¹ However, whilst offering a potentially sustainable solution for combined nutrient and CO₂ abatement, the process footprint can be up to two orders of magnitude greater than

that of the BNR process.¹ Optimization of the process, so as to enhance the CO₂ fixation (and so biomass growth) and nutrient assimilation, is thus critical.

Reported figures for the biomass-normalised CO₂ fixation rate, R_c' (Table 1) for a single species (*Anabaena sp.*) vary between 0.5 and 1.2 g CO₂ g biomass⁻¹ d⁻¹ for a gas stream containing ambient concentrations of CO₂,¹² the precise R_c' value being dependent on CO₂ concentration $C_{c,g}$,³ light intensity I ,¹² and other operating conditions such as hydraulic residence time (HRT). Corresponding figures for *B. braunii* indicate somewhat lower rates but a higher maximum attainable algal biomass concentration (X_{max}); reported data for *C. vulgaris* and *Scenedesmus obliquus* indicate moderate CO₂ fixation rates (0.09-0.35 and 0.098-0.26 g CO₂ g biomass⁻¹ d⁻¹ respectively) with corresponding maximum specific growth rates (μ_{max}) of 1.37 d⁻¹ and 1.19 d⁻¹.

Table 1

CO₂ fixation as a function of I appears to follow no recognisable pattern across either different species or different investigations for the same species.¹ Against this, for individual studies subject to the same standardized conditions fixation and biomass productivity both increase with I as expected to some maximum governed by light saturation.^{3,12,13} Batch experiments on four different algal species (*C. vulgaris*, *P. subcapitata*, *S. salina*, and *M. aeruginosa*) indicate that an approximate trebling of light intensity (from 36 $\mu\text{mol photons m}^{-2} \text{ s}^{-1}$) yields a 70-90% and 35-45% increase in biomass productivity and CO₂ uptake respectively¹⁴. Further increases in I may then inhibit and diminish R_c and μ .¹⁵

In the case of nutrient removal, a wide range of removals and biomass productivity (P_X) values for *C. vulgaris* have been reported (Table 2). PBR performance again increases with HRT and biomass concentration X , due to the limited nutrient uptake rate of the biomass, but is also pH-sensitive.¹⁶ A maximum uptake rate of 4-5 mg L⁻¹d⁻¹ N and 0.4-0.6 mg L⁻¹d⁻¹ P has been reported for both a classical stirred tank PBR and a membrane PBR operating at a 2-5 d

HRT.¹⁷ Nutrient removal for continuous processes of 2-3d HRT are generally below 85% for both N and P, compared to 75-88% N and 80-99% P for the BNR process¹. This reduced robustness compared with BNR arises primarily from the combined impact of the lower X_{max} (generally <1.5 g/L, cf. >3 gL⁻¹ for BNR) and slower algal biokinetics.

Table 2

Whilst various studies have reported trends in key parameters such as X and R_c , optimisation is complicated by the large number of variables, including light intensity, CO₂ gas or organic carbon (OC) liquid load, biomass concentration and volume, biomass retention time, algal species, biomass physico-chemistry (specifically pH and temperature) and feedwater nutrient load. To optimise the system for just five of the key variables for a single algal species and reactor configuration, based on just three parameter values and a classical n-factorial approach, would demand 243 (i.e. 3⁵) individual experiments.

An alternative to the classical factorial-based approach is the use of statistical experimental design to reduce the number of tests, and identify synergistic relationships and optimum conditions. This includes Box Behnken Design (BBD) which, while developed in the early 1960s¹⁸, has only recently been employed for algal bioreactor optimisation,¹⁹ in particular relating to lipid or biofuel generation.^{20,21} BBD permits a significant reduction in the number of experiments whilst still enabling synergies between the different parameters to be identified along with the optimum set of conditions.²² It therefore provides an elegant and efficient approach for elucidating inter-relationships for complex, multi-parameter systems, such as PBRs.

Given the practical significance and potential economic benefit of combined nutrient abatement and CO₂ fixation,¹ it is of obvious interest to evaluate this specific application more extensively. The current study appraises the influence of the most important process variables of influent gas CO₂ concentration, light intensity and temperature, along with feed

water N, P and TC, on the key performance determinants of biomass accumulation, CO₂ fixation rate, and nutrient removal. The study uniquely both (a) employs Box Behnken statistical experimental design to identify the optimum condition, and (b) combines nutrient abatement from wastewater with CO₂ fixation, potentially from flue gases, in a single practical experimental study. The use of BBD for this dual function enables the optimum conditions to be identified.

2 Material and Methods

2.1 Algae preparation and determination

The *Chlorella vulgaris* algal strain (CCAP 211/11B, CS-42) used was as described previously.²³ Experiments were conducted in 350 mL cylindrical glass columns (ID = 4 cm), each with a 250 mL working volume. The standard MLA medium consists of the following components: MgSO₄·7H₂O 49.4 mg/L; NaNO₃ 170 mg /l; K₂HPO₄ 34.8 mg /l; H₃BO₃ 2.47 mg/L; vitamin B₁₂ 0.05 μg /l; thiamine HCl 0.1 mg/L; biotin 0.05 μg/L; Na₂EDTA 4.56 mg/L; FeCl₃·6H₂O 1.58 mg/L; CuSO₄·5H₂O 0.01 mg/L; ZnSO₄·7H₂O 22 μg/L; CoCl₂·6H₂O 0.01 mg/L; NaMoO₄·2H₂O 0.006 mg/L; NaHCO₃ 16.9 mg/L; CaCl₂·2H₂O 29.4 mg/L). The concentrations of both NaNO₃ and K₂HPO₄ in the standard medium were varied to accommodate different concentrations of TN (0-56 mg L⁻¹), TP (0-19 mg L⁻¹). 250 ml batches of sterilized medium with different concentrations of TN (0-56 mg L⁻¹), TP (0-19 mg L⁻¹), and TC (0-20 mg L⁻¹) were inoculated by 1 vol% pre-cultured *C. vulgaris* with initial cells concentration of 0.7×10⁶ cells mL⁻¹. The culture was continuously fed with a flow of 50-52 mL min⁻¹ filtered air enriched with 0.03-22% CO₂, adjusted by digital mass flow controllers (MC-100SCM, Cole-Parmer, USA); inlet and outlet gas concentration ($C_{c,g}$) was measured using a CO₂ probable meter (G110, Geotech, UK). The control sample was aerated with air only (0.03 % CO₂). The cultivation temperature (T) was varied from ambient 30°C down to 20°C using an incubator refrigerator (Temperature Cycling Chamber, LABEC, Australia).

Continuous illumination at a light intensity (I) between 180 and 400 μE , provided by adjusting the number of 8W LED lights between 4 and 8, was measured by a light meter (LI-250A, LI-COR, US). A 5 mL sample was extracted daily for analysis, equating to a hydraulic and solids residence time of 50 days, and all runs lasted for 10-13 days.

Nutrient concentrations of the 0.45 μm -filtered liquid sample were determined colorimetrically using HACH test kits (DR/890 Colorimeter, HACH, USA) and the total organic carbon (TOC) concentration using a Shimadzu TOC analyser (TOC-VCPH, Shimadzu, Japan). The optical density was determined by UV-Vis spectrophotometer spectrophotometer (Jasco *V-670*, JASCO Corporation, Japan) at 680 nm, and the reading converted to dry cell weight (DCW g/L) by calibration. The specific growth rate μ was then calculated from the initial and final biomass concentrations and the corresponding cultivation time. For all nutrient tests the control sample contained 6 mg L^{-1} TP and 28 mg L^{-1} TN, based on the typical medium MLA composition stipulated by the supplier.

2.2 Experimental design and regression analysis

Box Behnken Design (BBD) was employed to optimize the process based on algal growth, expressed as μ in d^{-1} , biomass productivity P_X in g (dry weight) biomass $\text{L}^{-1} \text{d}^{-1}$, and:

- CO₂ capture (R_C), as a function of feed $C_{c,g}$, I , and T , and
- Nutrient removal, as a function of feedwater composition with reference to TN, TP and total carbon (TC).

R_C is given by $C P_X M_{\text{CO}_2}/M_C$, where C is the dried cells % carbon content, measured by an element analyser (CHNS/O analyser, PerkinElmer, USA), P_X the biomass productivity, and M_{CO_2} and M_C are the respective molar weights of CO₂ and carbon.

BBD experimental design employs a matrix of tests based on a number of parameters, in this case three. The impact of each parameter is evaluated by selecting three or more values (or “levels”) of these parameters and then conducting tests which encompass every combination of each parameter value. The results of the experiments in terms of the impacting (or “response”) parameters can then be evaluated through a statistical model.²² Two such multi-level, three-parameter BBD matrices were created to examine the synergistic relationships between these sets of three parameters within specific limits (Table 3). A total of 15 experimental runs, randomly sequenced in duplicate to reduce the effect of the temporal-related errors, were conducted to determine the 10 coefficients of the second order polynomial generated from the statistical model.²⁴ JMP statistical discovery software (SAS v11.2.1) was used to complete the regression analysis and generate the graphical relationships. The variability of the factors was expressed as coefficient of determination (R^2) values. The model equation was then used to identify the interaction between the variables within the specified experimental boundary conditions. Subsequent optimization to identify the conditions for maximising μ , R_c and nutrient removal was through maximising the desirability function using Derringer’s desired function (DDF) methodology.²⁵

Table 3

3 Results and discussion

3.1 Scoping trials: Growth as a function of CO₂ concentration

The specific growth rate μ at a fixed T of 24°C and I of 200 μE over a 10-day cultivation period increased from 0.64 d^{-1} ($R_c = 0.328 \text{ g L}^{-1} \text{ d}^{-1}$) for $C_{c,g} = 0.03\%$ to 1.17 d^{-1} at 5%, with a corresponding X_{max} of 2.94 g L^{-1} ($R_c = 0.744 \text{ g L}^{-1} \text{ d}^{-1}$) at the higher $C_{c,g}$ (Fig.1 a-c). Increasing $C_{c,g}$ further to 22% resulted in a decreased growth rate ($\mu = 0.097 \text{ d}^{-1}$, $X_{max} = 1.11 \text{ g L}^{-1}$, $R_c = 0.28 \text{ g L}^{-1} \text{ d}^{-1}$).

The reduced biomass production at the high $C_{c,g}$ of 22% is likely to be due to the inhibitive impact of the associated low pH on growth and CO_2 mass transfer, the latter pertaining to the relatively slow rate of hydrolysis of CO_2 to H_2CO_3 ,¹ and the associated depression of photosynthesis.^{26,27} Low-intermediate $C_{c,g}$ concentrations (0.03-5 %), on the other hand, caused insignificant inhibition: these levels were associated with pH values in the optimum range of 7-7.5. A 25% increase in μ (from 0.52 to 0.65 d^{-1}) has been previously reported on increasing $C_{c,g}$ from ambient levels to 15%, whilst reports^{2,28-30} have indicated that increasing $C_{c,g}$ from 2.5% to 9.5% has little influence on growth.

Fig. 1

3.2 Scoping trials: Growth and nutrient removal

Increasing the initial TN concentration ($\text{TN}_{\text{init}} = 0\text{-}56 \text{ mg L}^{-1}$) at a constant TP of 8 mg L^{-1} produced the expected increase in *C. vulgaris* biomass growth (Fig. 2) and with close to 100% TP removal within the TP_{init} range of $2.7\text{-}7 \text{ mg L}^{-1}$. Against this, the initial TP concentration apparently has a significant impact on algal growth and TN uptake, with only 30% N removal at the lowest TP_{init} concentration (1.2 mg L^{-1}). TN removal also declined from >90% to 75% removal at the highest TP_{init} concentration of 19 mg L^{-1} , where the corresponding TP removal also declined to 53%. The low removal efficiency (RE) can be largely attributed to the excessive nutrient load and/or its unbalanced N/P ratio (Fig. 3), along with the impairment of light transmission by the high biomass concentration. Whilst high TP concentrations generally favour biomass productivity,²⁸ studies conducted at a number of different N/P ratios (Table 2) have demonstrated that the ratio is crucial for effective nutrient removal. An optimum value of 8 has been reported³¹ – within the range of 7-10 found for the current study (Fig. 3) associated with a maximum specific growth rate of 1.04 d^{-1} .

Fig. 2

Fig. 3

3.3 Multiple regression analysis and analysis of variance

The multiple regression analysis conducted to determine the relationships between the three response parameters of R_C , N and P RE, and μ with respect to $C_{c,g}$, I and T generated the following second-order polynomial equations from the BBD matrix of experimentally-measured data (Table 4):

$$R_C, \text{ mg L}^{-1}d^{-1} = 4710 + 298 C_{c,g} - 2.93 I - 331 T + 0.0128 C_{c,g}I - 8.63 C_{c,g}T - 1.56 \times 10^{-3} IT - 0.965 C_{c,g}^2 + 3.23 \times 10^{-3} I^2 + 6.83 T^2 \quad (1)$$

$$\mu, d^{-1} = 2.02 + 0.216 C_{c,g} - 1.27 \times 10^{-4} I - 0.090 T - 3.60 \times 10^{-4} C_{c,g}I - 5.24 \times 10^{-4} C_{c,g}T - 2.36 \times 10^{-5} IT + 4.26 \times 10^{-3} C_{c,g}^2 + 1.18 \times 10^{-5} I^2 + 1.90 \times 10^{-3} T^2 \quad (2)$$

$$TN \text{ RE} (\%) = 41.2 + 9.33 C_{c,g} + 0.067 I + 3.00 T - 2.03 \times 10^{-17} C_{c,g}I - 0.040 C_{c,g}T + 1.42 \times 10^{-017} IT - 0.812 C_{c,g}^2 - 3.11 \times 10^{-4} I^2 - 0.060 T^2 \quad (3)$$

$$TP \text{ RE} (\%) = -32.2 - 1.71 C_{c,g} - 0.049 I + 11.5 T + 0.012 C_{c,g}I + 0.181 C_{c,g}T - 9.47 \times 10^{-18} IT - 0.589 C_{c,g}^2 - 3.88 \times 10^{-5} I^2 - 0.245 T^2 \quad (4)$$

The coefficient of determination (R^2) of the regression equations for the correlations for R_C , μ , and the RE values for TN and TP were 0.94, 0.98, 0.98 and 0.94 respectively (Fig. 4). The above quadratic expressions can thus adequately describe the relationship between the factors and responses.

Analysis of variance (ANOVA) was applied to generate the sum of squares, degree of freedom (df), mean squares, f-values and p-values by fitting the experimental results to the second-order polynomials Eqs. 1-4. P-values below 0.05, i.e. representing a significant

correlation, were generated for $C_{c,g}$ and I for μ , R_c , and TN and TP removal. The impact of T was found to be less significant (p-values > 0.1) within the range examined. Whilst the linear terms (i.e. terms in $C_{c,g}$ and I) were found to significantly influence μ (p-value<0.05), the combined terms (i.e. $C_{c,g}T$ and IT) were less significant. N and P removals were both significantly influenced by the individual and combined initial terms $C_{c,g}$ and I , whereas the influence of the $C_{c,g}T$ and IT terms was less significant. Similarly, for R_c there was better interaction between $C_{c,g}$ and T , but T itself remained insignificant in comparison with the other parameters. The satisfactory agreement found between the experimental and model data (Fig. 4), justified the use of the equations for generating the response surface correlations.

Fig. 4

Table 4

3.4 BBD analysis and optimization

3D response surface and 2D contour plots (Figs 5-6) were generated from Equations 1-4 for two factors ($C_{c,g}$, I), the third (T) being kept constant. The discrete data points refer to actual experimental response data values, added to demonstrate the fit with the model-generated response surface.

R_c increases with increasing $C_{c,g}$, between 0.03 and 5%, with I up to 100 μE (Fig. 5 a & b), corroborating previous studies³² reporting similar trends, but decreased with beyond 100 μE $m^{-2}s^{-1}$. Microalgal cells exposed to high light irradiance may undergo damage of the photosynthetic units, making them non-functional and causing photo-inhibition. Whilst this can take place at all irradiance levels, non-photochemical quenching (NPQ) processes become evident if the rate of photo-inhibition exceeds the rate of repair resulting in large proportions of the captured light being dissipated.³³ Conversely, as light irradiance decreases

the level of photosynthesis-active radiation decreases to low levels which significantly reduce photosynthesis activity, as reflected in the CO₂ fixation rates.

Generally, growth and metabolic rates are enhanced by increasing the temperature until an optimum value is reached for a species; further temperature increases may then reduce cell growth through cell damage or death.³⁴ For the current study the temperature range of 20-30°C selected was insufficiently broad to generate a significant change in R_c through either microbial or gas solubility impacts. The results recorded were nonetheless consistent with those previously reported,³⁵ and were reflected in the related parameter μ which demonstrated similar trends (Fig. 5 c & d).

TN RE followed a similar trend of increasing removal with increasing $C_{c,g}$ and decreasing I over the ranges studied (Fig. 6 a & b), with ~100% removal attained at a relatively low irradiance (50-200 μ E) and 3-5% $C_{c,g}$. TP trends indicated a flatter response with irradiation at the maximum $C_{c,g}$ of 5% (Fig. 6 c & d). TN uptake appears to be reduced at low CO₂ concentrations³⁶. Conversely, high CO₂ concentrations activate N reductase, enhancing N assimilation² as well as increasing the HCO₃⁻ concentration through reaction of CO₂ with protons generated from N and P uptake by microalgae cells.³⁷ This then maintains a neutral pH value, providing more favourable conditions for algal growth.

Figs. 5-6

TP was 100% removed at all irradiance levels studied at the highest $C_{c,g}$ of 5%, only demonstrating irradiance dependency at lower $C_{c,g}$ levels. Light stress associated with high light intensities arises, when the energy imparted cannot be dissipated as fluorescence and heat, can impair photosynthesis,³⁸ potentially breaching the light saturation limit of the alga and negatively impacting on P removed. Consumption of TP was accompanied by photosynthesis uptake of dissolved inorganic carbon. However, P removal is impacted more

than N removal by pH via abiotic precipitation, though assimilation by algae remains the primary P removal mechanism.³⁹ P removal close to 100% has been previously reported⁴⁰.

According to the BBD results, the optimal conditions for maximizing R_c , μ , and the TN and TP removal efficiencies based on DDF methodology were found to be at $C_{c,g} = 5\%$, $I = 100 \mu\text{E m}^{-2} \text{ s}^{-1}$ and $T = 22 \text{ }^\circ\text{C}$. Under these conditions, the predicted R_c , μ and TN, TP removal efficiencies were found to be $1000 \text{ mg L}^{-1} \text{ d}^{-1}$, 1.53 d^{-1} and 100% RE for both N and P respectively.

Table 5

4 Conclusions

The response of *Chlorella vulgaris* (C_v) to different levels of feed gas CO_2 concentration ($C_{c,g}$), light irradiation (I), Temperature (T), and aqueous nutrient concentrations (TN and TP) has been assessed. Response parameters comprised the specific growth rate μ , the CO_2 uptake rate R_c and nutrient removal efficiency (RE N and P).

Scoping trials revealed $C_{c,g}$ values of 22% to be deleterious to μ and R_c , as well as to nutrient RE . R_c and μ dropped 2.64 and 12 folds respectively when $C_{c,g}$ increased from 5 to 22%. This was attributed to both pH effects and impaired CO_2 mass transfer. It was further demonstrated that C_v in MLA medium with a starting concentration of 6 mg L^{-1} P and 28 mg L^{-1} N could completely remove the nutrients with high associated μ and R_c values (of 1.17 d^{-1} and $744 \text{ mg L}^{-1} \text{ d}^{-1}$ respectively) following 10 days of cultivation. R_c , μ , and nutrient removal rates were significantly decreased when the culture was fed with a feed gas containing 22% CO_2 .

Subsequent optimisation was based on a $C_{c,g}$ range of 0.03% (i.e. ambient levels) to 5%, along with a temperature range of 20-30°C and light intensity of 100-400 μE . A following experiment was then carried out to optimise nutrient removal within concentration ranges of 0-56 mg L^{-1} TN and 0-12 mg L^{-1} TP and 0-20 mg L^{-1} TC. Optimisation employed Box

Behnken design (BBD) and response surface method (RSM) to discern the nature of the synergies between operating parameters and concentrations of aqueous nutrient and CO₂ gas concentration.

The analysis revealed a synergy between $C_{c,g}$ and I for both R_c and μ , temperature having no significant effect. To achieve maximum CO₂ fixation rate with complete nutrient removal (N and P) and obtain a maximum μ of 1.53 d⁻¹, the analysis predicted optimum $C_{c,g}$ and I values of 5 % and 100 μ E respectively. This was confirmed through experimental validation. The R_c , μ and nutrient removal efficiencies appear to have been well described by quadratic models developed using BBD according to multiple linear regression analysis of the outputs, with ANOVA analysis confirming the relative importance of the different parameters.

ACKNOWLEDGEMENT

This work was made possible by the support of a National Priorities Research Programme (NPRP) grant from the Qatar National Research Fund (QNRF), grant reference number NPRP 6-1436-2-581. The statements made herein are solely the responsibility of the authors.

References

1. Judd S, van den Broeke LJ, Shurair M, Kuti Y, Znad H. Algal remediation of CO₂ and nutrient discharges: A review. *Water Research* **87**:356-366 (2015).
2. Cheng L, Zhang L, Chen H, Gao C. Carbon dioxide removal from air by microalgae cultured in a membrane-photobioreactor. *Separation and Purification Technology* **50(3)**:324-329 (2006).
3. Chiang C-L, Lee C-M, Chen P-C. Utilization of the cyanobacteria *Anabaena* sp. CH1 in biological carbon dioxide mitigation processes. *Bioresource Technology* **102(9)**:5400-5405 (2011).
4. Lam MK, Lee KT. Effect of carbon source towards the growth of *Chlorella vulgaris* for CO₂ bio-mitigation and biodiesel production. *International Journal of Greenhouse Gas Control* **14**:169-176 (2013).
5. Basu S, Roy AS, Mohanty K, Ghoshal AK. CO₂ biofixation and carbonic anhydrase activity in *Scenedesmus obliquus* SA1 cultivated in large scale open system. *Bioresource Technology* **164**:323-330 (2014).
6. Solovchenko A, Gorelova O, Selyakh I, Semenova L, Chivkunova O, Baulina O, Lobakova E. *Desmodesmus* sp. 3Dp86E-1—a novel symbiotic chlorophyte capable of growth on pure CO₂. *Marine Biotechnology* **16(5)**:495-501(2014).
7. Wahal S, Viamajala S. Maximizing algal growth in batch reactors using sequential change in light intensity. *Applied Biochemistry and Biotechnology* **161(1-8)**:511-522(2010).
8. Béchet Q, Shilton A, Guieysse B. Modeling the effects of light and temperature on algae growth: State of the art and critical assessment for productivity prediction during outdoor cultivation. *Biotechnology Advances* **31(8)**:1648-1663 (2013).
9. Giannelli L, Yamada H, Katsuda T, Yamaji H. Effects of temperature on the astaxanthin productivity and light harvesting characteristics of the green alga *Haematococcus pluvialis*. *Journal of Bioscience and Bioengineering* **119(3)**:345-350 (2015).
10. Bosch FM, Lootens, H., Van -Vaerenbergh, E. The elimination of phosphates and nitrates of waste water by algal cultures. *Natuurwetensch T* (1974).
11. Maher C, Neethling J, Murthy S, Pagilla K. Kinetics and capacities of phosphorus sorption to tertiary stage wastewater alum solids, and process implications for achieving low-level phosphorus effluents. *Water Research* **85**:226-234 (2015).
12. Sánchez FJ, González-López C, Ación FF, Fernández SJ, Molina GE. Utilization of *Anabaena* sp. in CO₂ removal processes: modelling of biomass, exopolysaccharides productivities and CO₂ fixation rate. *Applied Microbiology and Biotechnology* **94(3)**:613-624(2012).

13. Gonçalves A, Simões M, Pires J. The effect of light supply on microalgal growth, CO₂ uptake and nutrient removal from wastewater. *Energy Conversion and Management* **85**:530-536 (2014).
14. Pires J, Gonçalves A, Martins F, Alvim-Ferraz M, Simões M. Effect of light supply on CO₂ capture from atmosphere by *Chlorella vulgaris* and *Pseudokirchneriella subcapitata*. *Mitigation and Adaptation Strategies for Global Change* **19**(7):1109-1117 (2014).
15. Fernández FGA, González-López C, Sevilla JF, Grima EM. Conversion of CO₂ into biomass by microalgae: how realistic a contribution may it be to significant CO₂ removal? *Applied Microbiology and Biotechnology* **96**(3):577-586 (2012).
16. Sutherland DL, Turnbull MH, Broady PA, Craggs RJ. Effects of two different nutrient loads on microalgal production, nutrient removal and photosynthetic efficiency in pilot-scale wastewater high rate algal ponds. *Water Research* **66**:53-62(2014).
17. Marbelia L, Bilad MR, Passaris I, Discart V, Vandamme D, Beuckels A, Muylaert K, Vankelecom IF. Membrane photobioreactors for integrated microalgae cultivation and nutrient remediation of membrane bioreactors effluent. *Bioresource Technology* **163**:228-235(2014).
18. Box GE, Behnken DW. Some new three level designs for the study of quantitative variables. *Technometrics* **2**(4):455-475(1960).
19. Kasiri S, Abdulsalam S, Ulrich A, Prasad V. Optimization of CO₂ fixation by *Chlorella kessleri* using response surface methodology. *Chemical Engineering Science* **127**:31-39 (2015).
20. Ghosh S, Roy S, Das D. Improvement of Biomass Production by *Chlorella* sp. MJ 11/11 for Use as a Feedstock for Biodiesel. *Applied Biochemistry and Biotechnology* **175**(7):3322-3335 (2015).
21. Skorupskaite V, Makareviciene V, Levisauskas D. Optimization of mixotrophic cultivation of microalgae *Chlorella* sp. for biofuel production using response surface methodology. *Algal Research* **7**:45-50(2015).
22. Montgomery DC. Design and analysis of experiments. John Wiley & Sons; (2008).
23. Alketife AM, Znad H, Judd S. Synergistic effects and optimization of nitrogen and phosphorus concentrations on the growth and nutrient uptake of a freshwater *Chlorella vulgaris*. *Environmental Technology* (2016).
DOI:[10.1080/09593330.2016.1186227](https://doi.org/10.1080/09593330.2016.1186227)
24. Raffin M, Germain E, Judd S. Optimising operation of an integrated membrane system (IMS)—A Box–Behnken approach. *Desalination* **273**(1):136-141(2011).
25. Harrington E. The desirability function. *Industrial quality control* **21**(10):494-498 (1965).

26. Silva HJ, Pirt SJ. Carbon dioxide inhibition of photosynthetic growth of *Chlorella*. *Journal of General Microbiology* **130(11)**:2833-2838(1984).
27. Sung K-D, Lee J-S, Shin C-S, Park S-C, Choi M-J. CO₂ fixation by *Chlorella* sp. KR-1 and its cultural characteristics. *Bioresource Technology* **68(3)**:269-273(1999).
28. Choi HJ, Lee SM. Effect of the N/P ratio on biomass productivity and nutrient removal from municipal wastewater. *Bioprocess and Biosystems Engineering* **38(4)**:761-766(2015).
29. Ruiz-Martinez A, Martin Garcia N, Romero I, Seco A, Ferrer J. Microalgae cultivation in wastewater: Nutrient removal from anaerobic membrane bioreactor effluent. *Bioresource Technology* **126(0)**:247-253(2012).
30. Fu W, Gudmundsson O, Feist AM, Herjolfsson G, Brynjolfsson S, Palsson BØ. Maximizing biomass productivity and cell density of *Chlorella vulgaris* by using light-emitting diode-based photobioreactor. *Journal of Biotechnology* **161(3)**:242-249(2012).
31. Karapinar Kapdan I, Aslan S. Application of the Stover–Kincannon kinetic model to nitrogen removal by *Chlorella vulgaris* in a continuously operated immobilized photobioreactor system. *Journal of Chemical Technology and Biotechnology* **83(7)**:998-1005(2008).
32. E. Purba T. CO₂ reduction and production of algal oil using microalgae *Nannochloropsis oculata* and *Tetraselmis chuii*. *Chem. Eng. Trans.* **21**:397–402 (2010).
33. Perrine Z, Negi S, Sayre RT. Optimization of photosynthetic light energy utilization by microalgae. *Algal Research* **1(2)**:134-142 (2012).
34. Raven JA, Geider RJ. Temperature and algal growth. *New phytologist* 441-461(1988).
35. Taucher J, Jones J, James A, Brzezinski M, Carlson C, Riebesell U, Passow U. Combined effects of CO₂ and temperature on carbon uptake and partitioning by the marine diatoms *Thalassiosira weissflogii* and *Dactyliosolen fragilissimus*. *Limnology and Oceanography* **60(3)**:901-919 (2015).
36. Vilchez C, Vega JM. Nitrite uptake by *Chlamydomonas reinhardtii* cells immobilized in calcium alginate. *Applied Microbiology and Biotechnology* **41(1)**:137-141(1994).
37. Redfield AC. The influence of organisms on the composition of sea-water. *The sea* 26-77 (1963).
38. Wilhelm C, Jakob T. From photons to biomass and biofuels: evaluation of different strategies for the improvement of algal biotechnology based on comparative energy balances. *Applied Microbiology and Biotechnology* **92(5)**:909-919 (2011).

39. Su Y, Mennerich A, Urban B. Coupled nutrient removal and biomass production with mixed algal culture: Impact of biotic and abiotic factors. *Bioresource Technology* **118(0)**:469-476(2012).
40. Ji M-K, Abou-Shanab RAI, Kim S-H, Salama E-S, Lee S-H, Kabra AN, Lee Y-S, Hong S, Jeon B-H. Cultivation of microalgae species in tertiary municipal wastewater supplemented with CO₂ for nutrient removal and biomass production. *Ecological Engineering* **58(0)**:142-148 (2013).
41. Sydney EB, Sturm W, de Carvalho JC, Thomaz-Soccol V, Larroche C, Pandey A, Soccol CR. Potential carbon dioxide fixation by industrially important microalgae. *Bioresource Technology* **101(15)**:5892-5896 (2010).
42. Ruangsomboon S. Effect of light, nutrient, cultivation time and salinity on lipid production of newly isolated strain of the green microalga, *Botryococcus braunii* KMITL 2. *Bioresource Technology* **109(0)**:261-265 (2012).
43. Honda R, Boonnorat J, Chiemchaisri C, Chiemchaisri W, Yamamoto K. Carbon dioxide capture and nutrients removal utilizing treated sewage by concentrated microalgae cultivation in a membrane photobioreactor. *Bioresource Technology* **125**:59-64 (2012).
44. Tang D, Han W, Li P, Miao X, Zhong J. CO₂ biofixation and fatty acid composition of *Scenedesmus obliquus* and *Chlorella pyrenoidosa* in response to different CO₂ levels. *Bioresource Technology* **102(3)**:3071-3076 (2011).
45. Ruiz-Marin A, Mendoza-Espinosa LG, Stephenson T. Growth and nutrient removal in free and immobilized green algae in batch and semi-continuous cultures treating real wastewater. *Bioresource Technology* **101(1)**:58-64 (2010).
46. Ho S-H, Chen W-M, Chang J-S. *Scenedesmus obliquus* CNW-N as a potential candidate for CO₂ mitigation and biodiesel production. *Bioresource Technology* **101(22)**:8725-8730 (2010).
47. Abou-Shanab RAI, Ji M-K, Kim H-C, Paeng K-J, Jeon B-H. Microalgal species growing on piggery wastewater as a valuable candidate for nutrient removal and biodiesel production. *Journal of Environmental Management* **115(0)**:257-264 (2013).
48. López CG, Fernández FA, Sevilla JF, Fernández JS, García MC, Grima EM. Utilization of the cyanobacteria *Anabaena* sp. ATCC 33047 in CO₂ removal processes. *Bioresource Technology* **100(23)**:5904-5910 (2009).
49. De Godos I, Mendoza J, Ación F, Molina E, Banks C, Heaven S, Rogalla F. Evaluation of carbon dioxide mass transfer in raceway reactors for microalgae culture using flue gases. *Bioresource Technology* **153**:307-314 (2014).
50. Gao F, Yang Z-H, Li C, Zeng G-M, Ma D-H, Zhou L. A novel algal biofilm membrane photobioreactor for attached microalgae growth and nutrients removal from secondary effluent. *Bioresource Technology* **179**:8-12 (2015).

51. Lee SH, Jo BH, Park JY, Oh HM. Increased microalgae growth and nutrient removal using balanced N: P ratio in wastewater. *Journal of Microbiology and Biotechnology* **23(1)**:92-98 (2013).
52. Boonchai R, Seo GT, Seong CY. Microalgae photobioreactor for nitrogen and phosphorus removal from wastewater of sewage treatment plant. *International Journal of Bioscience, Biochemistry and Bioinformatics* **2(6)**:407 (2012).
53. Lau P, Tam N, Wong Y. Wastewater nutrients removal by *Chlorella vulgaris*: optimization through acclimation. *Environmental Technology* **17(2)**:183-189(1996).
54. Silva-Benavides AM, Torzillo G. Nitrogen and phosphorus removal through laboratory batch cultures of microalga *Chlorella vulgaris* and cyanobacterium *Planktothrix isothrix* grown as monoalgal and as co-cultures. *Journal of Applied Phycology* **24(2)**:267-276(2012).
55. Feng Y, Li C, Zhang D. Lipid production of *Chlorella vulgaris* cultured in artificial wastewater medium. *Bioresource Technology* **102(1)**:101-105(2011).

Figures Captures

Fig. 1: Algal growth trends with feed gas CO₂ concentration: (a) X, (b) P_x, (c) R_c', and (d) R_c.

“Control” refer to the sample aerated with only air (0.03%), ($I=200 \mu\text{mol m}^{-2} \text{s}^{-1}$, $T=24 \text{ }^\circ\text{C}$).

Fig.2: X_{max} and % nutrient removal, 13 days cultivation, at different initial nutrient concentrations (TN_{init} and TP_{init}): normalised initial nutrient concentration = initial nutrient concentration / maximum initial nutrient concentration (TN_{init,max} and TP_{init,max} = 56 and 19 mg L⁻¹ respectively).

Fig.3: Specific growth rate and nutrient removal efficiencies after 13 days of cultivation and a function of N/P concentration ratio.

Fig.4: Comparison between experimental data and predicated values of R_c, TN and TP removal, and μ . The dotted curved lines indicate the >95% confidence bands; horizontal dotted lines represent the mean of the Y leverage residuals (i.e. the measure of agreement with the model).

Fig. 5: 3D response surface and contour map for CO₂ fixation rate (a ,b) and μ (c ,d), at the optimum temperature of 22 °C.

Fig. 6: 3D response surface and contour map for TN RE (a, b) and TP RE (c, d), at the optimum temperature of 22 °C.

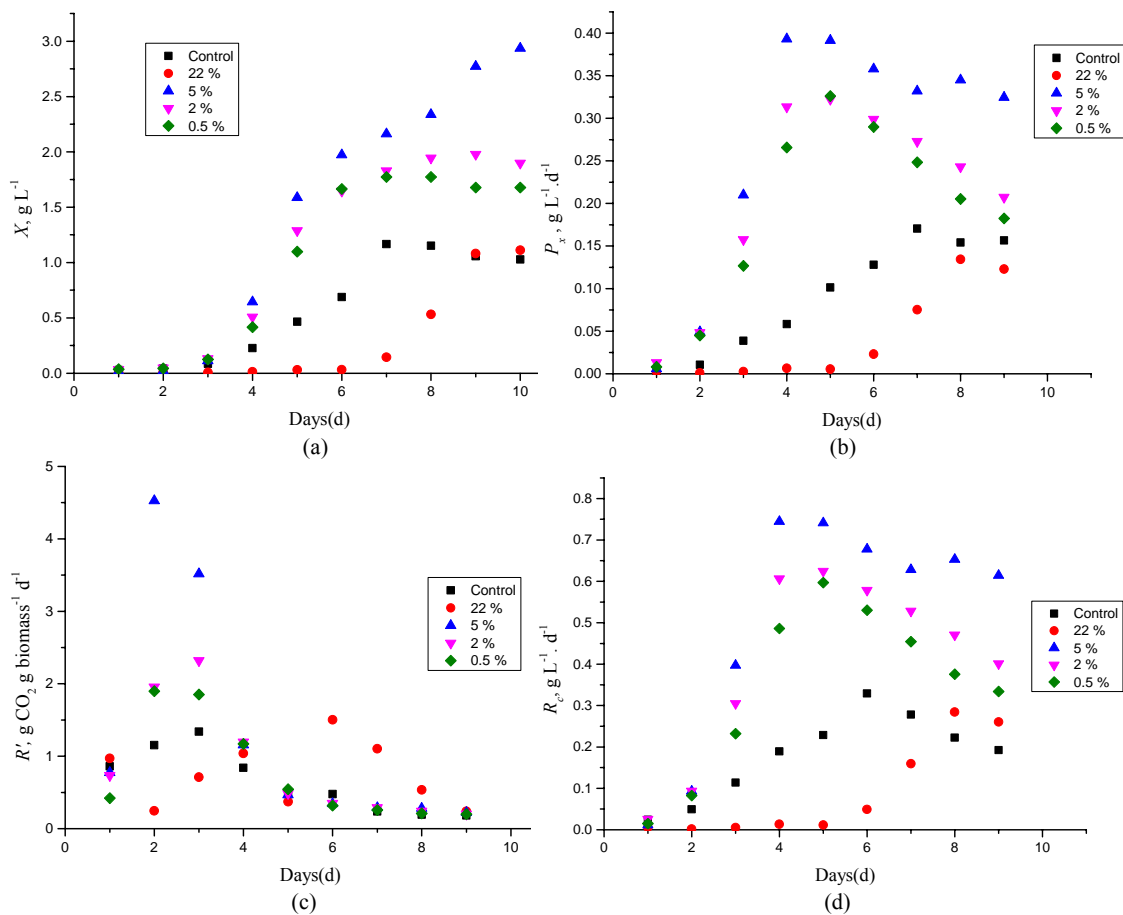


Fig. 1: Algal growth trends with feed gas CO₂ concentration: (a) X , (b) P_x , (c) R_c' , and (d) R_c .

“Control” refer to the sample aerated with only air (0.03%), ($I=200 \mu\text{mol m}^{-2} \text{s}^{-1}$, $T=24 \text{ }^\circ\text{C}$).

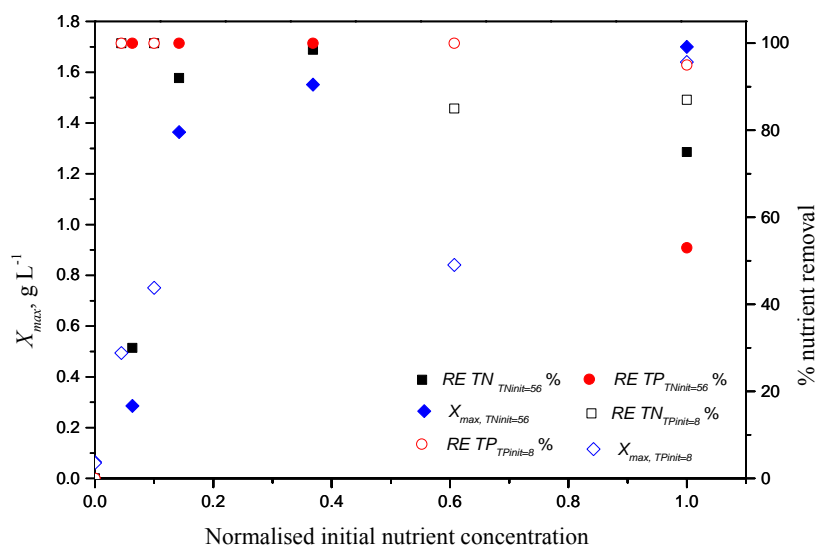


Fig. 2: X_{max} and % nutrient removal, 13 days cultivation, at different initial nutrient concentrations (TN_{init} and TP_{init}): normalised initial nutrient concentration = initial nutrient concentration / maximum initial nutrient concentration ($TN_{init,max}$ and $TP_{init,max}$ = 56 and 19 $mg L^{-1}$ respectively).

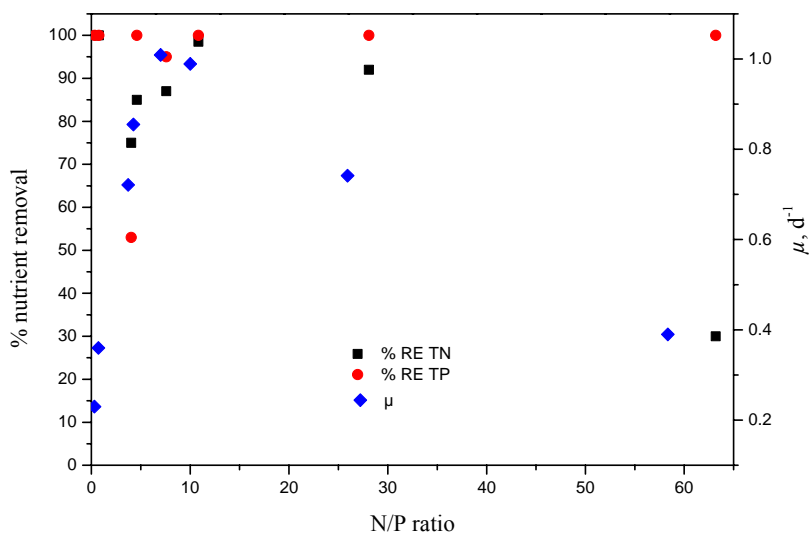


Fig. 3: Specific growth rate and nutrient removal efficiencies after 13 days of cultivation and a function of N/P concentration ratio.

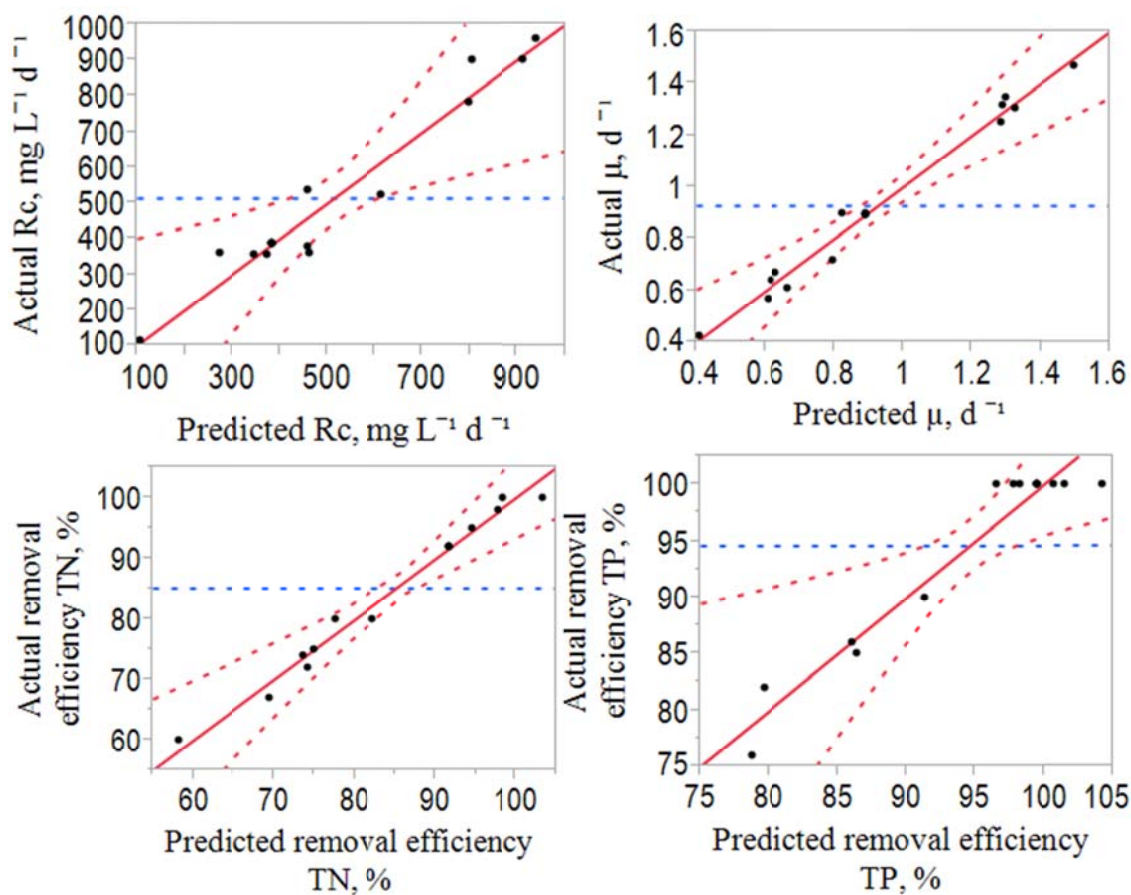


Fig. 4: Comparison between experimental data and predicted values of R_c , TN and TP removal, and μ . The dotted curved lines indicate the >95% confidence bands; horizontal dotted lines represent the mean of the Y leverage residuals (i.e. the measure of agreement with the model).

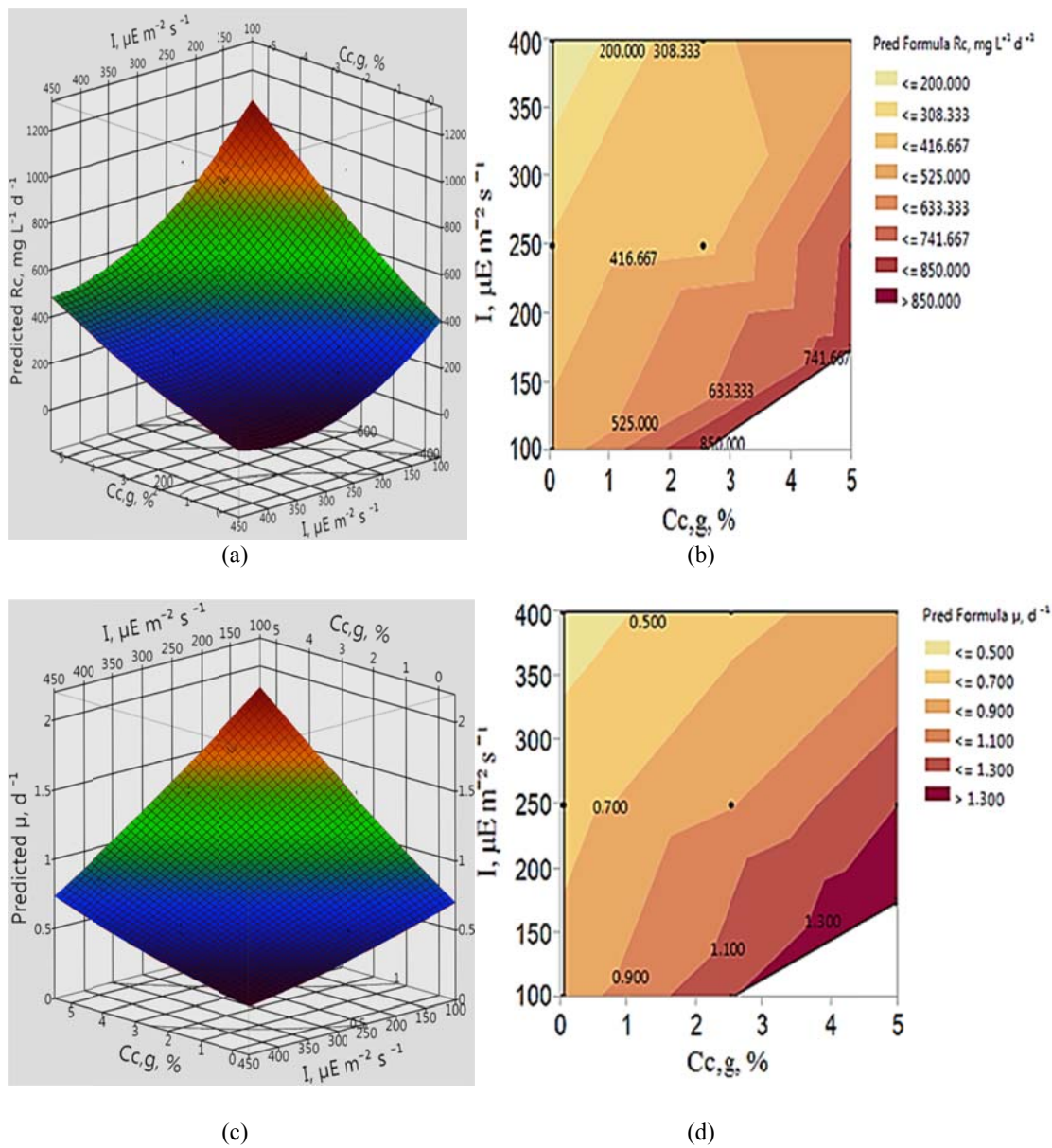


Fig. 5: 3D response surface and contour map for CO₂ fixation rate (a, b) and μ (c, d), at the optimum temperature of 22 °C.

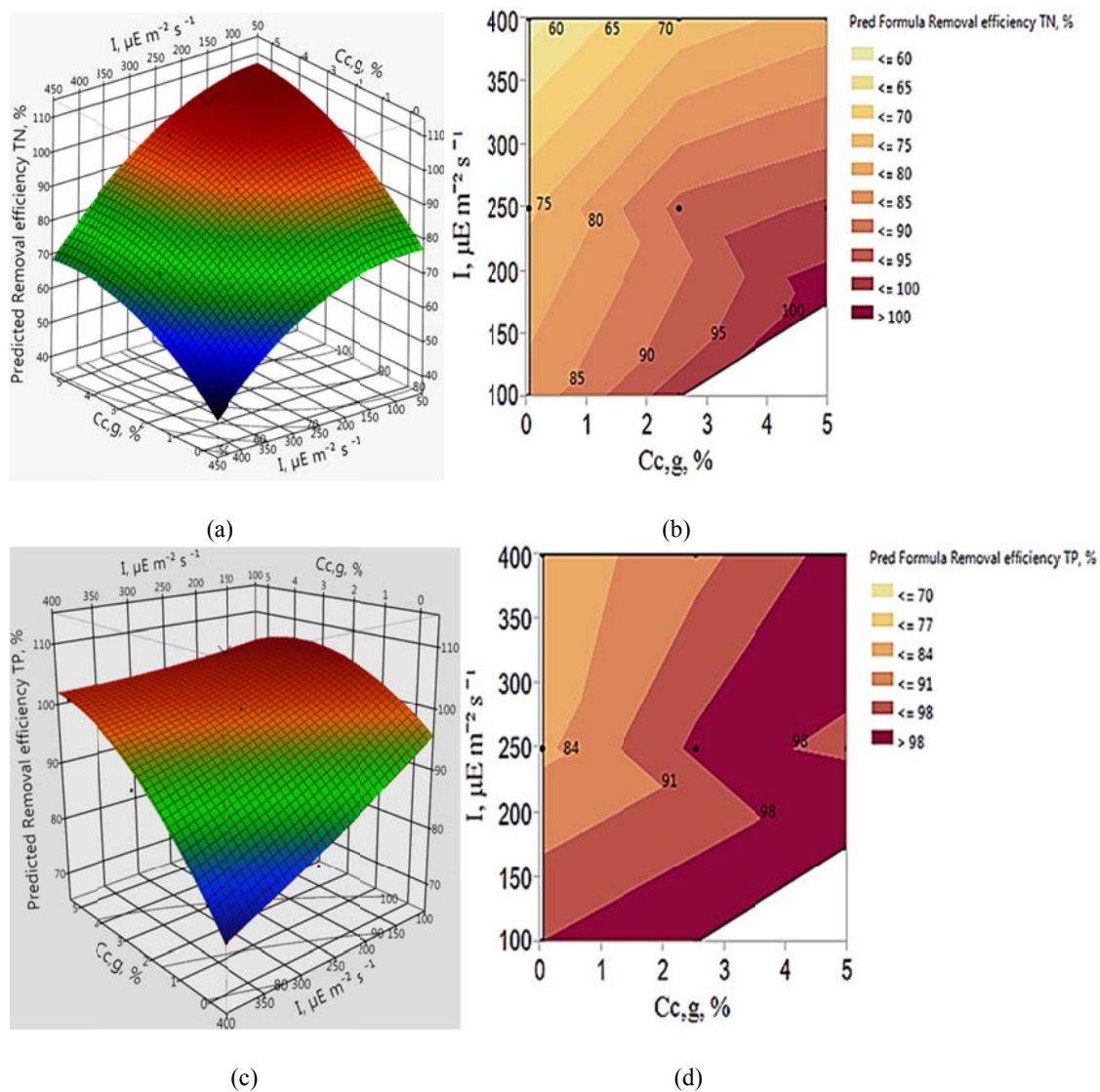


Fig. 6: 3D response surface and contour map for TN RE (a, b) and TP RE (c, d), at the optimum temperature of 22 °C.

Tables Captures

Table 1: Reported CO₂ fixation rates for various algae species, batch systems unless otherwise stated.

Table 2: Variation of the TP and TN removal efficiencies with the optimum N/P ratio.

Table 3: Parameter values.

Table 4: BBD matrix, experimental outputs.

Table 5: Comparison between predicted and experimental optimum conditions.

Table 1: Reported CO₂ fixation rates for various algae species, batch systems unless otherwise stated.

Light intensity, $\mu\text{mol m}^{-2} \text{s}^{-1}$	CO ₂ fixn. rate, R_c , $\text{g L}^{-1} \text{d}^{-1}$	HRT, d	Max. biomass concn, X_{max} , g L^{-1}	Inlet CO ₂ $C_{c,g}$, %v/v	Flow rate Q_g , vvm	R_c' , $\text{g CO}_2 \text{g biomass}^{-1} \text{d}^{-1}$	Specific growth rate μ , d^{-1}	Refs
<i>Botryococcus braunii</i>								
62.5	0.496	53	3.11	5	--	0.15	0.24	
87.5-538	0.089	2.5	1.9	0.03 ^a	--	0.047	--	42
570	0.024	1 ^b	0.92	1	--	0.026	0.052	43
<i>Scenedesmus obliquus</i>								
107	0.097	0.8-0.2	1.39	0.03 ^a -35	2.1-8.3	0.06	0.64	5
180	0.28	--	1.84	0.03 ^a -50	0.25	0.15	0.94	44
135-200	--	1	--	0.03 ^a	--	--	0.28	45
60	0.549	--	3.5	10	0.003	0.15	1.19	46
40-50	0.08**	33	0.3	15	2	0.26	1.14	40
40	0.049**	--	0.53	0.03 ^a	--	0.098	--	47
<i>Anabaena sp.</i>								
900	1.45	2-3 ^b	3	0.03 ^a	0.2	0.48	--	48
0-460	0.43	3.3 ^b	0.76	10.6	$\sim 3 \times 10^{-4}$	0.56	--	49
250	0.65-0.8	5	0.58-1.2	5-15, 10	0.04	0.66-1.12	--	3
650	0.16-0.58	0.7-6 ^b	0.35-0.95	0.03 ^a	0.13-0.75	0.45-0.61	--	12
975	0.25-0.65	0.7-6 ^b	0.45-1.35	0.03 ^a	0.13-0.75	0.55-0.48	--	
1625	0.36-1	0.7-6 ^b	0.5-2	0.03 ^a	0.13-0.75	0.72-0.5	--	
<i>Chlorella vulgaris</i>								
180	0.47	100	1.34	0.03 ^a	--	0.35	1.19	13
62.5	0.25	53	1.94	5	--	0.12	0.29	41
126	0.30	--	0.821	0.03 ^a	--	0.36	0.73	14
(60-70)	0.162	--	0.75	(0.03 ^a -5)	--	0.21	0.28	4
(40-50)	0.062**	33	0.29	15	2	0.21	1.37	40
40	0.046**	--	0.49	0.03 ^a	--	0.094	--	47
142	0.12**	2 ^b	1.37	4	0.014	0.09	--	50

^aAtmospheric level; HRT = hydraulic residence time; vvm = volume gas per volume liquid per minute.

^bContinuous system otherwise Batch system.

** R_c estimated from Chisti ratio: $\text{CO}_{0.48}\text{H}_{1.83}\text{N}_{0.11}\text{P}_{0.01}$; $R_c = 1.88 \times P_{\text{overall}}$, $P_{\text{overall}} = \Delta X/\Delta t$.

Table 2: Variation of the TP and TN removal efficiencies with the optimum N/P ratio.

<i>Cultivation wastewater</i>	<i>Strain</i>	<i>Optimum N/P ratio</i>	<i>TP % removal</i>	<i>TN% removal</i>	P_X ($mg L^{-1} d^{-1}$)	<i>Ref</i>
Domestic	Mixed	14	92.4	77	--	51
Domestic	<i>C. vulgaris</i>	192.6	84.2	44	--	52
Domestic	<i>C. vulgaris</i>	1-10	89	78	2.75	28
		11-20	81	84	2.3	
		21-30	59	83	1.18	
		61-70	24	73	0.41	
Synthetic	<i>C. vulgaris</i>	8	--	93	--	31
Domestic	<i>C. vulgaris</i>	2.85	97.8	67.2	234	29
Synthetic	<i>C. vulgaris</i>	18.8	85.9	82.5	72	50
Domestic	<i>C. vulgaris</i>	7	70	86	--	53
Municipal	<i>C. vulgaris</i>	21	100	70	54	54
	Co-culture ¹		100	80	65	
Synthetic	<i>C. vulgaris</i>	5	96	97	230-212	55

¹ *C. vulgaris* & *Planktothrix*

Table 3:Parameter values

<i>Parameters</i>	<i>Range of values</i>	
	<i>Min</i>	<i>Max</i>
<u><i>CAMPAIGN 1</i></u>		
%CO ₂ <i>C</i> _{c,g} , v/v	0.04	5
Light intensity <i>I</i> , μE	100	400
Temperature <i>T</i> , °C	20	30
<u><i>CAMPAIGN 2</i></u>		
TC, mg L ⁻¹	0	20
TN, mg L ⁻¹	0	56
TP, mg L ⁻¹	0	12

Table 4:BBD matrix, experimental outputs.

Run	C_{cg} , %	I , $\mu\text{E m}^{-2}$ s^{-1}	T , C°	TN RE , %	TP RE , %	μ , d^{-1}	R_C , mg L^{-1} d^{-1}
1	5	250	20	98	100	1.30	958
2	2.5	250	25	92	100	0.89	386
3	0.04	250	30	74	76	0.64	358
4	2.5	400	30	67	86	0.56	357
5	2.5	400	20	72	90	0.61	363
6	0.04	250	20	75	85	0.67	363
7	0.04	100	25	80	100	0.72	377
8	2.5	250	25	92	100	0.89	386
9	5	400	25	80	100	0.9	539
10	2.5	250	25	92	100	0.9	386
11	2.5	100	30	100	100	1.35	899
12	5	175	25	100	100	1.47	72
13	5	250	30	95	100	1.25	525
14	0.04	400	25	60	50	0.42	112
15	2.5	100	20	100	100	1.32	900

Table 5: Comparison between predicted and experimental optimum conditions

<i>Factors</i>	<i>Response</i>	<i>Experimental</i>	<i>Predicted</i>	<i>% error</i>
$C_{c,g} = 5 \%$	$R_C \text{ g L}^{-1} \cdot \text{d}^{-1}$	1032	1000	3.4
$I = 100 \mu E$	μ, d^{-1}	1.51	1.53	1.4
$T = 22^\circ\text{C}$	RE TN, %	96	100	4.0
	RE TP, %	100	100	0.0